

Observed and calculated gravity anomalies above a tunnel driven in clays – implication for errors in gravity interpretation

Vratislav Blecha^{1*} and David Mašín¹

¹*Institute of Hydrogeology, Engineering Geology and Applied Geophysics, Faculty of Science, Charles University in Prague, Czech Republic*

* Corresponding author: vblecha@natur.cuni.cz

ABSTRACT

The aim of this work was to evaluate gravity effect of deformation zone, which forms around subsurface cavities and to assess which method of the density determination of soils in the surveyed area is optimal. We measured and modeled gravity anomaly above the tunnel excavated in stiff clays. Technical parameters of the tunnel were known. The shape of deformation zone around the tunnel was determined by geotechnical modelling. Material parameters of clays necessary for geotechnical model were obtained from measurement of borehole samples in soil mechanics laboratory. For calculation of gravity anomaly of the tunnel we used densities of clays derived from laboratory measurements of borehole samples. The fit between observed and calculated gravity data was not accurate in this case, however. The reason probably was that volume and water content in the borehole clay samples changed after their removal from the depth. Better fit was obtained when we used densities derived from gamma-gamma well log. We found that the gravity effect of the deformation zone that forms around the tunnel in stiff clays is negligible (0.001 mGal). In our case, concrete tunnel lining has a bigger influence on the amplitude of the anomaly than the deformation zone (0.008 mGal). When we neglect the lining in the interpretation, we obtain an error of 20% in the estimate of the tunnel depth.

INTRODUCTION

Gravimetry is often the leading method used in geophysical surveys of the subsurface cavities and undermined areas (e.g. Banham and Pringle 2011; Bishop *et al.* 1997; Butler 1984; Debeglia *et al.* 2006; Eppelbaum 2011; Ghatge 1993; Rybakov *et al.* 2001). Results of gravity surveys show that we can often localize old mine workings in the depths where they should

not be located according to the results of preliminary investigation. The reason is that the roof of old galleries is gradually collapsing so that the empty space is moving closer to the surface. Moreover, a narrow elliptical deformation zone, which is formed above collapsing mine workings, is a source of an additional negative gravity anomaly (Blecha and Mrlina 2001). Such a complex anomaly is difficult to interpret quantitatively.

The existence of a deformation zone above the old mine workings suggests that a similar deformation zone forms also around the newly mined workings and this zone could affect the gravity anomaly. We decided to verify this fact by gravity measurements over railway tunnel driven in clays. We chose tunnel in clays because soils (unlike hard rocks) constitute environment without strong discontinuities, which may be represented reliably by an advanced geotechnical model. Gravity model of the deformation zone around the tunnel was then derived from the geotechnical modelling.

In order to correctly interpret the gravity measurements, it is important to know precisely the density conditions at the location. Primarily, we decided to use densities measured and calculated from geotechnical parameters necessary for construction of a numerical model of the tunnel. A special 22 m deep borehole was drilled directly at the site of gravity survey and geotechnical parameters were determined from drill core samples. During the work on the project it turned out that it might be beneficial to apply different methods for calculating the densities, and based on the fit of the measured and modeled gravity data to choose the optimal method of density determination.

As a subject of our survey we chose the railway tunnel excavated in Tertiary clays and claystones near the village Brezno in the Northern part of the Czech Republic. The tunnel was 1758 m long with inner cross section of 43.7 m². The maximum thickness of overburden was 25 m. Apart from relatively homogeneous clayey sediments, small seams of coal or coal-claystones occasionally occurred in the tunnel profile. The tunnel was excavated by the so-called prevault construction procedure. Thickness of the concrete tunnel lining was 60 cm on the walls and 120 cm on the bottom. The tunnel excavation started in 2000 and has been completed in 2007, after delays caused by unexpected collapse of the tunnel in 2003. For more details on the tunnel construction, see Heřt (2007).

FIELD MEASUREMENTS

Two 100 m long gravity profiles have been traced out perpendicular to the axis of the tunnel at a distance of 130 and 160 meters from the southern portal. The roof of the tunnel is 12.5 m and the bottom of the tunnel is 20 m below the surface on the profile P1 . On the profile P2 the tunnel is 1 m deeper in comparison with profile P2. For the field measurement of gravity we used gravimeter Scintrex CG-3M with resolution of 0.001 mGal. The distance between gravity stations was 5 m. Tidal effects and long-term linear drift is removed by internal software of gravimeter. Residual drift was registered by reoccupation of base station in a time interval of 1 hour. 20% of field gravity stations were measured repeatedly at different times and after correction for residual drift measuring error was calculated. The mean square error of measurements was 0.004 mGal. Relative Bouguer anomalies were calculated from measured values of gravity. Bouguer anomalies were separated into the regional and residual parts. The terrain relief in the vicinity of the gravity profiles was very flat and no topographical features influenced the amplitude and shape of residual anomaly caused by the tunnel. Gravity effect of the remote topography on the 100 m long profile was constant. It was removed by the process of regional/residual separation and should, therefore, not affect the residual gravity anomaly caused by the tunnel. Positions of the gravity profiles relative to the position of the tunnel southern portal and boreholes used for obtaining the soil samples and density log are shown in Fig. 1.

Results of field measurements above the tunnel are in Fig. 2a (profile P1) and in Fig. 2b (profile P2). Negative gravity effect of the tunnel is masked by high linear regional gradient in Bouguer anomalies. Rising values of Bouguer anomalies towards SE are in accord with regional gravity map (Sedlák 2000). This trend is caused by deep geological structure, because the area of study is on the boundary between negative gravity area of Krušné hory/Erzgebirge Mts. in NW and positive gravity area of Teplá-Barrandian unit in SE. The regional linear trend includes also the gravity effect of remote topographical masses. The gravity effects of topographic features outside the survey area generally will have spatial wavelengths larger than that of the target anomaly. Therefore, the topographic features outside the survey area can be treated as components of the local regional field variation and corrected in a single regional-residual field separation step (Butler 1980, 1985; Yule 1998). Linear equations of regional trend were calculated from non-anomalous areas of gravity profiles P1 and P2 (0-20 m and 80-100 m) and subtracted from Bouguer anomalies. The

resulting residual anomaly with amplitude of -0.046 mGal on profile P1 was subject of further modelling.

DENSITY MEASUREMENTS

Detailed knowledge of the density of the soil massif is crucial for the development of a gravity model of the underground cavity. We applied three methods of density determination: two laboratory methods and one “in situ” method. Soil samples for laboratory measurements were collected from a 22 m deep borehole drilled in the SE end of the gravity profile P1. Well logging was carried out in the other borehole at 120 m distance from gravity profile P1 (Fig. 1). This borehole was drilled during the survey of the tunnel route (Zima *et al.* 2001).

Soil mechanics laboratory

First set of densities were measured in the soil mechanics laboratory. Densities were calculated from measurements made for the construction of a geotechnical numerical model of the tunnel. Interval of drill core sampling was 1 m. For geotechnical modelling, an important variable is void ratio e defined as a ratio of volume of voids vs. volume of mineral grains. The following formulas are the basic equations of soil mechanics reported e.g. in Holz and Kovacs (1981) or in Craig (2004). Values of void ratio e can be calculated according to the formula

$$e = \frac{D_G w_m}{S} \quad (1)$$

where D_G is the density of soil grains, w_m is gravimetric water content and S is the degree of saturation. Gravimetric water content w_m is defined as the ratio of the mass of water in the soil sample M_W to dry soil sample mass M_D

$$w_m = \frac{M_W}{M_D} \quad (2)$$

The degree of saturation S represents the proportion of pores filled with water and it is calculated as the ratio of water volume w_v and porosity P

$$S = \frac{W_v}{P} \quad (3)$$

In Eq. (3), w_v is a volumetric water content defined as the ratio of the volume of water in the soil sample V_W to dry soil sample volume V_D .

$$w_v = \frac{V_W}{V_D} \quad (4)$$

Porosity P is the ratio of volume of voids in the soil sample to volume of the entire sample and with void ratio e it is defined as follows:

$$P = \frac{e}{1 + e} \quad (5)$$

Densities of soils in natural conditions D_N were calculated according to the formula

$$D_N = (1 - P) D_G + PS \quad (6)$$

The last equation is valid only in case that pores are filled with water with density of 1000 kg/m³. Values of void ratio e could be linearized with depth for purpose of geotechnical modelling (see Fig. 3, curve b). We therefore used linearized values of D_N also for the gravity model of the tunnel.

Triple weighing method

The second set of measurements of density of soil samples was obtained in the laboratory specialized in determination of rocks and soils densities. The method applied is so called “triple weighing” (Kobr 1997). Soil sample with mass of about 200 g is dried up at temperature of 105 °C to constant mass (M_1). Subsequently, the sample is inserted into a desiccator and vacuumed. Then, directly in the desiccator, the sample is impregnated with distilled water or with some other suitable fluid (kerosene in case of clays). Impregnated samples are weighted in selected fluid (M_2) and finally in the air (M_3). From these three weighings it is possible to calculate grain density D_G , dry bulk density D_{DB} and porosity P according to the following equations

$$D_G = \frac{M_1 D_F}{M_1 - M_2} \quad (7)$$

$$D_{DB} = \frac{M_1 D_F}{M_3 - M_2} \quad (8)$$

$$P = \frac{1 - D_{DB}}{D_G} \quad (9)$$

where D_F is density of fluid used. The proper value of natural density D_N to use in gravity interpretations will depend upon the depth of the formation relative to the water table. In most cases, including as a rule those in which the depth of the water table is unknown, the wet bulk density D_{WB} is used (Grant and West, 1965). If the soil in natural conditions is fully saturated with water we can calculate natural density D_N according to formula

$$D_N = D_{WB} = D_{DB} + P \quad (10)$$

Values of calculated natural densities varied with the depth within a very narrow range (Fig 3, curve a), linear interpolation of densities with depth showed almost no variation, and we therefore used constant (average) value of density for gravity modelling of the tunnel in this case.

Gamma-gamma well logging

The third method used for density determination was gamma-gamma well logging. Gamma-gamma logs, also called density logs, are records of the radiation from a gamma source in the probe after it is attenuated and backscattered in the borehole and surrounding rocks. The logs can be calibrated in terms of bulk density under the proper conditions and converted to porosity if grain and fluid densities are known. The density log comes from a borehole that is different from the borehole from which the soil samples were collected, but both boreholes were drilled in the immediate vicinity of the gravity profile P1 (Fig. 1).

The results of density measurements are shown in Fig. 3. Since the boreholes B1, B2 and the gravity profile are in different altitudes and sedimentary layers are horizontal in the area of our study, density curves in Fig. 3 are related to the center of the gravity profile (above the tunnel center). It is evident that density-depth curves from well log (curve c) and soil mechanics laboratory (curve b) are similar. A significant difference between curve b) and c) in Fig. 3 amounts to a systematic shift of densities by about 150 kg/m^3 . Density measurement in soil mechanics laboratory is based on water content determination of soil samples. Therefore, samples were collected from the centre of the drill core soon after its removal from the borehole and immediately wrapped into several layers of plastic foil. In spite of this careful handling, clay core sample probably did not retain the natural water content and

volume in the time interval between its withdrawal from the borehole and the measurement in the laboratory.

The measurement of densities in rock density laboratory was carried out on the same drill core samples as in the case of soil mechanics laboratory, but later in terms of time. The measurement of densities is based on mass determination of dry and fully impregnated samples, therefore the loss of natural wetness itself wouldn't be a problem in this case. But the density-depth curve a) in Fig. 3 differs substantially from curves b) and c). This is likely due to volume changes of soil samples. The clays are liable to shrinking while drying (losing water), and the calculated values of open porosity P are therefore likely underestimated and resulting values of natural densities are overestimated.

MODELLING

Geotechnical modelling

An unknown in the evaluation of the geophysical data is often the question of specific gravity decrease within the deformation zone around a cavity. To clarify this issue, geotechnical model capable of predicting porosity variation within the soil has been set up. The calculations were performed using the finite element method. For calculations, finite element program Tochnog Professional (Rodemann 2012) was used. Material parameters of soil samples from 22 m deep borehole were measured in the soil mechanics laboratory. The following laboratory experiments were performed for the characterization of the soil behavior:

Four undrained triaxial tests with measurement of pore water pressure (CIUP) on undisturbed soil samples

- Two isotropic compression tests on reconstituted soil samples
- Five shear box tests on undisturbed soil samples
- Three ring shear tests on reconstituted soil samples
- Two oedometric tests on undisturbed soil samples
- One oedometric test on reconstituted sample

The soil behavior was characterized by the hypoplastic constitutive model for clays (Mašín 2005). This is an advanced constitutive model, which takes into account the influence of void ratio e on soil behavior and properly captures non-linearity of the soil behaviour. The latter is

manifested in a continuous dependency of stiffness on the stress level and on the history of deformation. These aspects cannot be captured by the usually adopted models based on the theory of elasto-plasticity. It has been shown in a number of studies that the hypoplastic model is capable of correct predictions of a displacement fields around the tunnels (Mašín 2009; Svoboda *et al.* 2010). It has also been used for predicting the behavior of lumpy soil of similar granulometry and from the same sedimentary basin as is encountered in the location of the Březno tunnel (Najser *et al.* 2012). The calibration of material parameters is described in Brunát *et al.* (2009). In order to provide information needed to ensure replicability of the analyses, the parameter values are summarized in Tab. 1. Their explanation is, however, outside the scope of the present paper and interested readers are referred to the original publication (Mašín 2005).

In the modelling we used an enhanced version of the hypoplastic model allowing for predictions of the soil behaviour in the very small strain range (Niemunis and Herle 1997). Laboratory experiments required to calibrate the additional parameters were not performed. Instead, these parameters were taken from Svoboda *et al.* (2010), who studied clay of similar properties as the clay of the Březno tunnel. The additional parameters are summarized in Tab. 2. They are provided for the same reason as parameters of the basic hypoplastic model (Tab. 1). For the explanation of these additional parameters, see Niemunis and Herle (1997).

The model has been calculated using simplified 2D analyses based on so-called load reduction method. The load reduction parameter has been selected so that the numerical model gives predictions of the displacement field around the tunnel similar to those obtained from measurement. This procedure has been shown to provide a good estimate of the displacement field around the tunnel when compared to the fully 3D simulations (Svoboda and Mašín 2011). The initial conditions of the analyses comprised of vertical stresses (calculated from the soil and water unit weight), horizontal stresses (assumed to be equal to vertical stresses), and void ratio (estimated using the procedures outlined above). The analyses were performed as coupled deformation – ground water flow analyses, which means that excess pore water pressures were allowed to develop in agreement with the soil permeability, estimated as 10^{-10} m/s for the present clay. Fig. 4 shows contours of vertical and horizontal displacements predicted by the model. Comparison of the predictions with geotechnical monitoring data is in Fig. 5. Fig. 5a shows surface settlements, Fig. 5b gives the distribution of vertical displacement with depth in a vicinity of the tunnel. The match between

the model predictions and monitoring is from the perspective of geotechnical modelling generally very good. The agreement in predictions of displacement field gives an indirect indication that the geotechnical model is capable of predicting also variation of dry soil density during the course of tunnel excavation.

Gravity modelling

The distribution of void ratios calculated by the geotechnical model on profile P1 has been converted into wet bulk densities by assuming 86% degree of saturation S and density of mineral grains $D_G = 2650 \text{ kg/m}^3$. Gravity effect of the tunnel has been calculated as 2.5-D model with the lengths of 130 m towards SW (distance to the southern portal of the tunnel) and 1630 m towards NE (distance to the northern portal of the tunnel), but in our case gravity response of 2.5-D model is identical with 2-D model. For computation of gravity models we used GM-SYS profile modelling program (GM-SYS modelling 2012).

The tunnel modeled in clays with densities derived from geotechnical reference model is in Fig. 6. Wet bulk densities were calculated from soil laboratory measurements of borehole samples. Difference between amplitudes of observed and calculated anomalies is 0.014 mGal, error of modelling is 0.009 mGal. Error of modelling is mean square error calculated from differences between observed and calculated data.

Fig. 7 shows the results of the model when the deformation zone around the tunnel is considered. The shape of the deformation zone and variation of dry density is predicted by the geotechnical model. The difference between amplitudes of observed and calculated anomalies is 0.013 mGal, error of modelling is 0.008 mGal. Comparing this to the model in Fig. 6 it is clear that the gravity effect of deformation zone is very low (+ 0.001 mGal) and could be neglected in gravity interpretation (see Fig. 11 presented later). This result is in agreement with results of modelling of hypothetical tunnel in soft and stiff clays (Blecha and Mašín 2007). According to this work the gravity effect of the deformation zone in stiff clays is negligible and does not affect the measured gravity anomaly over the tunnel.

Fig. 8 presents model with constant density of 2170 kg/m^3 . This value of natural density is calculated from measurements of borehole samples in rock density laboratory. The fit between observed and calculated data is poor in this case. The difference between amplitudes is 0.022 mGal and error of modelling is 0.013 mGal.

The next figure (Fig. 9) shows the results of the model with densities measured directly in the borehole (gamma-gamma log). In this case, the difference between the amplitudes of observed and calculated anomalies is 0.003 mGal and error of modelling is 0.006 mGal. The fit between observed and calculated data is, therefore, very good for this model.

As the last step in our modelling we decided to evaluate the gravity effect of the concrete lining of the tunnel. The model in Fig. 10 is the same model as in Fig. 9, except that the tunnel lining with density of 2300 kg/m^3 is omitted. The difference between the amplitudes of calculated gravity anomalies in Fig. 9 and Fig. 10 implies that the gravity effect of the lining is 0.008 mGal. Disregarding the lining causes an error amounting to 20 % (2.5 m) in the tunnel depth estimation (see Fig. 11e).

In the process of modelling we tried to achieve the optimal match between the calculated and observed data. Only Model 4 (Fig. 9) provides a satisfactory level of fit between measured and modeled data. To reach the same fit for the other density models (the difference between amplitudes of observed and calculated anomalies 0.003 mGal and error of modelling is 0.006 mGal), we have to model the tunnel in an incorrect depth. This is demonstrated in Fig. 11.

CONCLUSIONS

The primary aim of our study was to determine whether the deformation zone that forms in the rocks around underground caverns and mine workings has a measurable gravity effect and whether it affects the accuracy of the interpretation of gravity data. Results of geotechnical and gravity modelling showed that the gravity effect of the deformation zone, which forms around the tunnel excavated in stiff Tertiary clays, is very small (0.001 mGal in our case) and impact on the accuracy of gravity interpretation is negligible. During the work on the project it turned out that the density obtained using conventional laboratory methods leads to modeled gravity effects that do not correspond well to measurements. When we used values of densities determined in the laboratory conditions for gravity modelling, we overpredicted the gravity effect and depth of the tunnel. The error depends on the laboratory method applied. Triple-weighing method gave the worst results. This can be caused by shrinkage of the soil sample during the measurement process. When we used the density specified by this laboratory method for gravity modelling, we estimated the depth of the tunnel with an error of 48% (roof in 18.5 m instead of the correct 12.5 m). The laboratory method based on the

determination of the natural water content of fresh samples gave better results. Using densities determined by this laboratory method we obtained an error of 24% in the estimated depth of the tunnel (roof in 15.5 m instead of the correct 12.5 m). The best fit was obtained using density determination by means of gamma-gamma well logging. When using the densities from the gamma-gamma log we estimated the depth of the tunnel in 13 meters (error of 4%). The estimation error in this case corresponds to the error of measurement of gravity.

We also calculated gravity effect of tunnel concrete lining. This effect is not negligible in our case (0.008 mGal). When we omit tunnel lining in our modelling we estimate the roof of the tunnel to lie in the depth of 15 m instead of the correct 12.5 m. Errors in the estimated depth of the tunnel for different density models are presented in Fig. 11.

It is obvious that during majority of standard geophysical surveys it is not possible to drill special boreholes, to measure gamma-gamma well logs, or to take soil samples and measure the density in the laboratory. Nevertheless, geophysicists should be aware of large errors which may arise in interpretation if they were to use only rough estimates of the density of the rock environment. This study shows a particular example.

We measured and modeled gravity anomaly above the tunnel driven in stiff Tertiary clays. Nevertheless, we conjecture that our results and conclusions relating to methods of density determination and gravity effect of deformation zone are valid for any relatively fresh mine working or cavern excavated in soils and soft rocks.

ACKNOWLEDGEMENTS

The authors gratefully acknowledge the support of the Ministry of Education, Youth and Sports of the Czech Republic (project MSM 0021620855) and the Czech Science Foundation (grants No. 205/07/0574 and P105/12/1705)

REFERENCES

Banham S.G. and Pringle J.K. 2011. Geophysical and intrusive site investigations to detect an abandoned coal-mine access shaft, Apedale, Staffordshire, UK. *Near Surface Geophysics* **9**, doi:10.3997/1873-0604.2011028.

Bishop I., Styles P., Emsley S.J. and Ferguson N.S. 1997. The detection of cavities using the microgravity technique: case histories from mining and karstic environments. In: *Modern Geophysics in Engineering Geology*, pp 155–168. Geological Society Engineering Group, Special Publication No. 12. Geological Society, London.

Blecha V. and Mrlina J. 2001. Microgravity prospecting for the voids in an abandoned coal-working field. *Proceedings of 7th European Meeting of Environmental and Engineering Geophysics*, Birmingham, UK.

Blecha V. and Mašín J. 2007. Gravity effects of deformation zones induced by tunneling in soft and stiff clays. *Proceedings of 13th European Meeting of Environmental and Engineering Geophysics*, Istanbul, Turkey.

Brunát, Z., Mašín, D. and Boháč, J. 2009. Parameters of a hypoplastic model for numerical model of Březno tunnel. *Proceedings of 37th Conference Zakládání Staveb*, Brno, Czech Republic, 187-192, (in Czech).

Butler, D. K. 1980. Microgravimetric techniques for geotechnical applications: *US Army Engineers Waterways Experiment Station Misc. Paper*, GL-80-13.

Butler D.K. 1984. Microgravimetric and gravity gradient techniques for detection of subsurface cavities. *Geophysics* **49**, 1084–1096.

Butler, D. K. 1985. Topographic effects considerations in microgravity surveying, in Proc. International Meeting on Potential Fields in Rugged Topography. Institute de Geophysique, *IGL Bull.* No. 7, 34-40.

Craig R.F. 2004. *Craig's Soil Mechanics*. 7th edn. Spon Press, Taylor & Francis Group, London and New York.

Debeglia N., Bitri A. and Thierry P. 2006. Karst investigations using microgravity and MASW; Application to Orléans, France. *Near Surface Geophysics* **4**, 215-225

Eppelbaum L.V. 2011. Review of environmental and geological microgravity applications and feasibility of their implementation at archaeological sites in Israel. *International Journal of Geophysics*, doi: 10.1155/2011/927080, ID 927080, 1-9.

Ghatge S.L. 1993. Microgravity method for detection of abandoned mines in New Jersey. *Bulletin of the Association of Engineering Geologists* **30**, 79–85.

GM-SYS modelling (2012). Accessed on June 11, 2012, at <http://www.geosoft.com/products/gm-sys>.

Google maps (2012), Accessed on January 15, 2012, at <https://maps.google.com/>.

Grant F. S. and West G. F. 1965. *Interpretation Theory in Applied Geophysics*. McGraw-Hill, New York.

Heřt, J. 2007. Březno tunnel construction. *Tunel*, **6**, 51-60, (in Czech).

Holtz R.D. and Kovacs W.D. 1981. *An Introduction to Geotechnical Engineering*. Prentice-Hall, Inc., Englewood Cliffs, New Jersey.

Kobr M. 1997. *Petrophysics*. Charles University, Karolinum, Prague, (in Czech)

Mašín D. 2005. A hypoplastic constitutive model for clays. *International Journal for Numerical and Analytical Methods in Geomechanics* **29**, 311-336.

Mašín D. 2009. 3D modelling of a NATM tunnel in high K_0 clay using two different constitutive models. *ASCE Journal of Geotechnical and Geoenvironmental Engineering* **135**, 1326-1335.

Najser, J., Mašín, D. and Boháč, J. 2012. Numerical modelling of lumpy clay landfill. *International Journal for Numerical and Analytical Methods in Geomechanics* **36**, 17-35.

Niemunis A. and Herle I. 1997. Hypoplastic model for cohesionless soils with elastic strain range. *Mechanics of Cohesive-Frictional Materials* **2**, 279–299.

Rodemann D. 2012. Tochnog Professional user's manual. Accessed on June 15, 2012, at <http://www.feat.nl>.

Rybakov M., Goldshmidt V., Fleischer L. and Rotstein Y. 2001. Cave detection and 4-D monitoring: a microgravity case history near the Dead Sea. *The Leading Edge* **20**, 896–900.

Sedlák J. 2000. Gravity map of the Czech Republic 1:200 000, sheet M-33-XIV Teplice. Geofyzika a.s. Brno.

Svoboda T. and Mašín D. 2011. Comparison of displacement fields predicted by 2D and 3D finite element modelling of shallow NATM tunnels in clays. *Geotechnik* **34**, 115-126.

Svoboda T., Mašín D. and Boháč J. 2010. Class A predictions of a NATM tunnel in stiff clay. *Computers and Geotechnics* **37**, 817-825.

Yule D.E., Sharp M.K. and Butler D.K. 1998. Microgravity investigations of foundation conditions. *Geophysics* **63**, 95-103

Zima J., Horčíčka R. and Vojíš M. 2001. Rerouting of railroad track Březno – Chomutov. Geologické služby s.r.o. Unpublished manuscript, (in Czech).

Figures

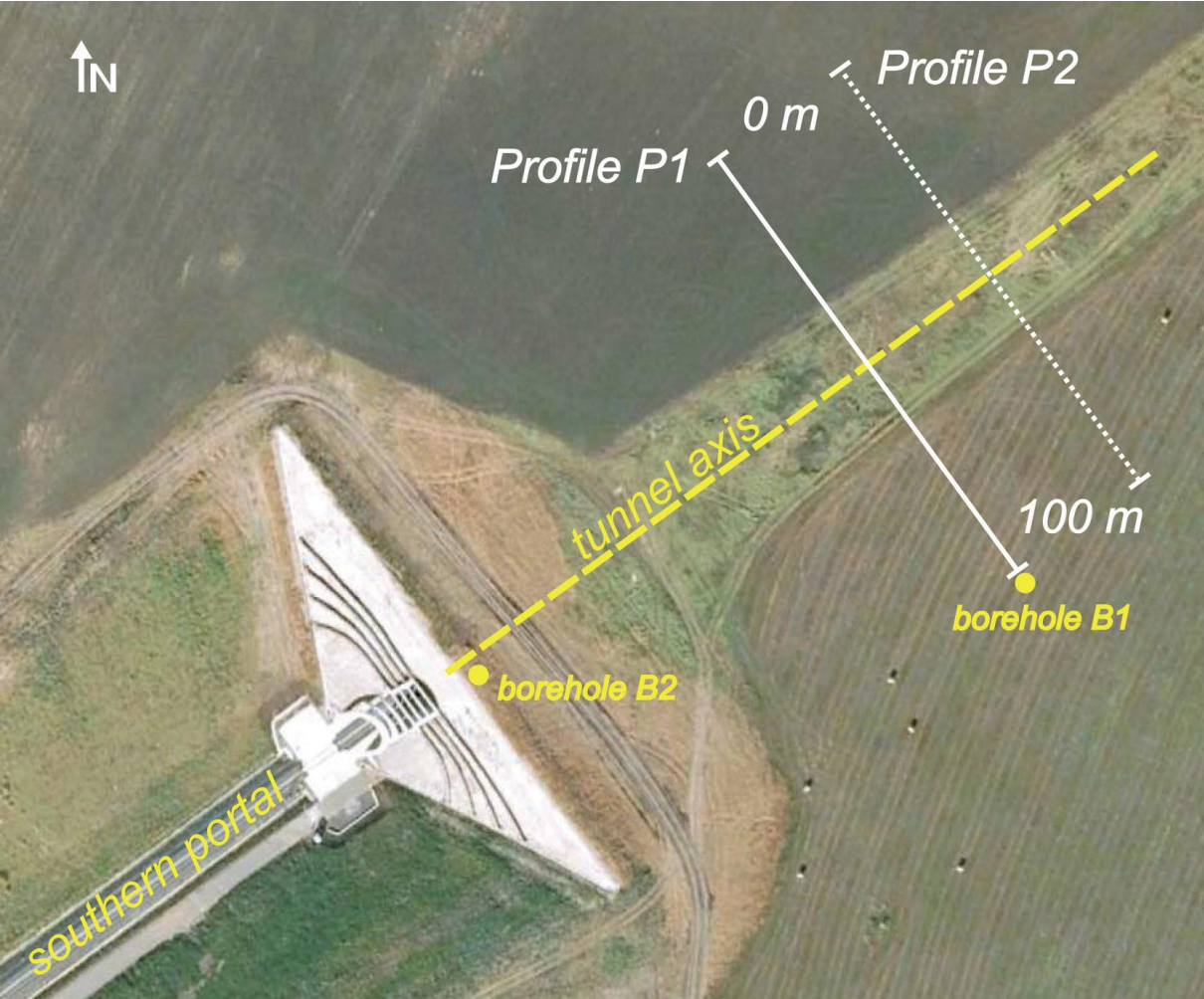
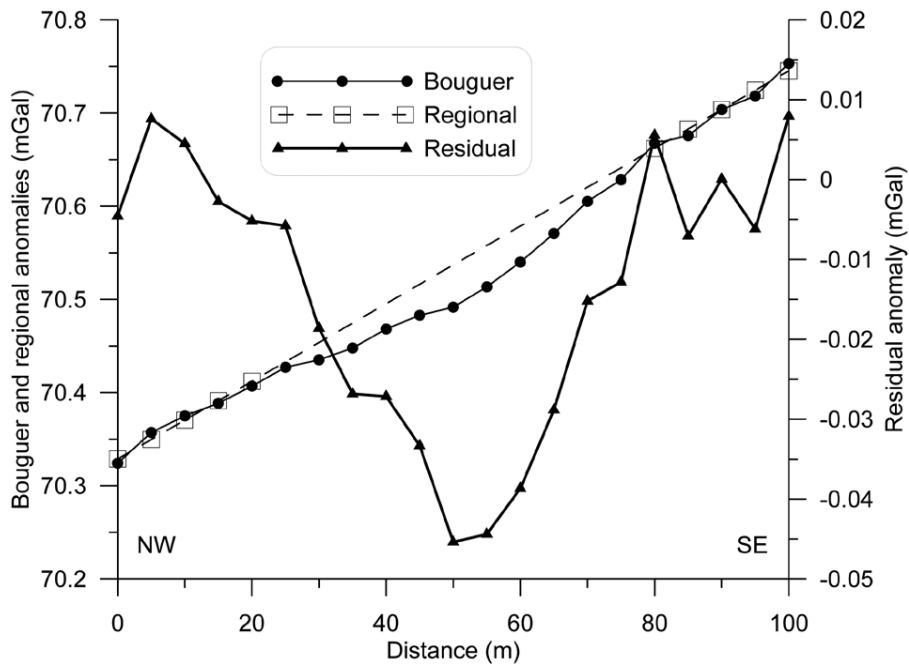


Figure 1. Location of gravity profiles P1, P2 and boreholes used for extraction of soil samples (B1) and gamma-gamma density log (B2). Situation relative to the tunnel southern portal. Satellite photo: Google maps (2012).

a)



b)

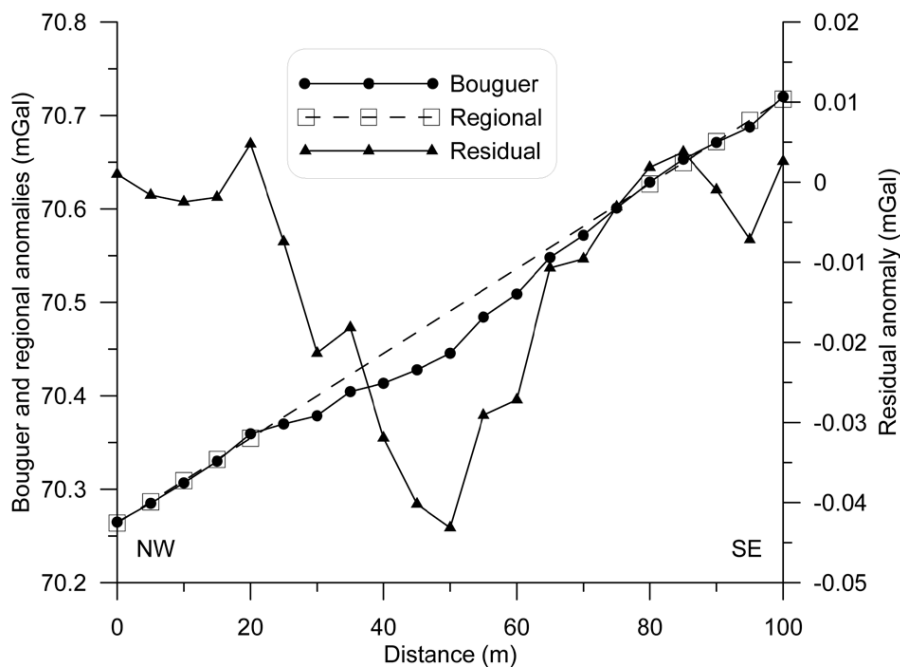


Figure 2. Results of gravity field measurements above the tunnel – (a) profile P1, (b) profile P2. Residual anomaly on profile P1 is modeled in Figures 6 – 10.

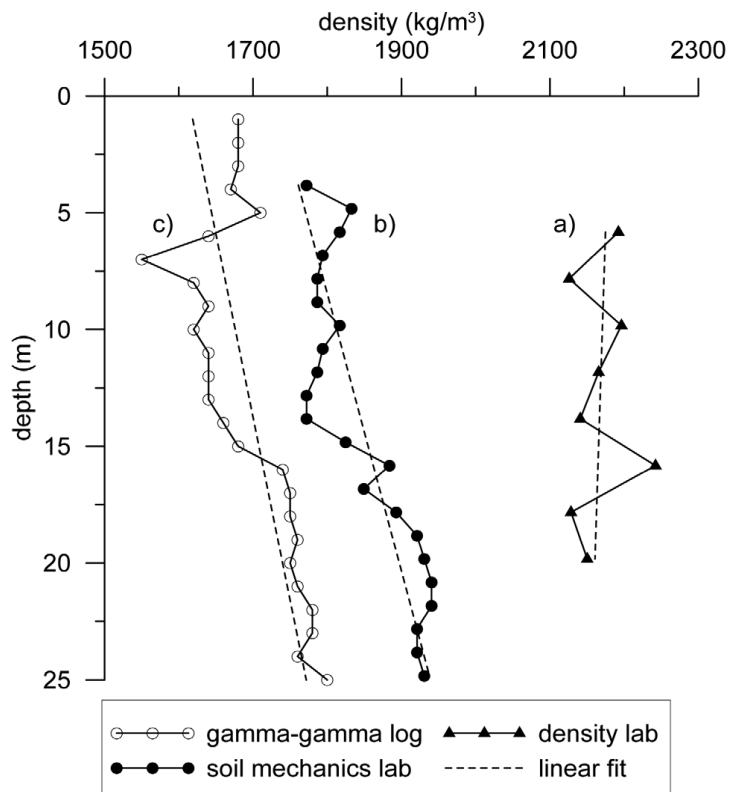


Figure 3. Results of density measurements. Plot of natural densities of clays D_N measured: a) in rock density laboratory (triple-weighing method), b) in soil mechanics laboratory (based on natural wetness measurement), c) in situ with gamma-gamma well logging.

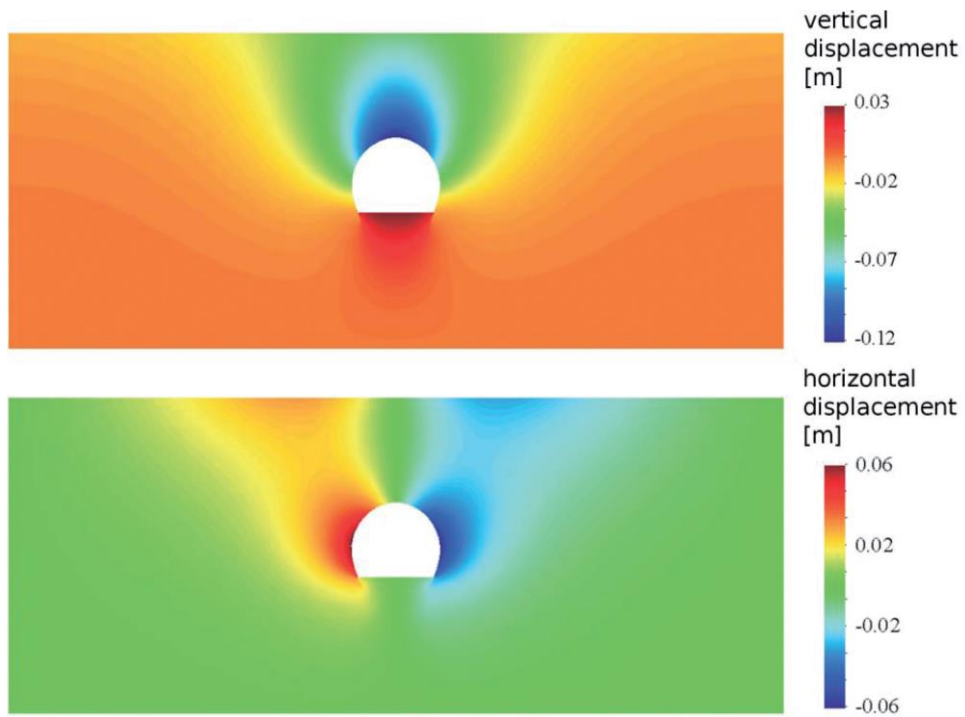
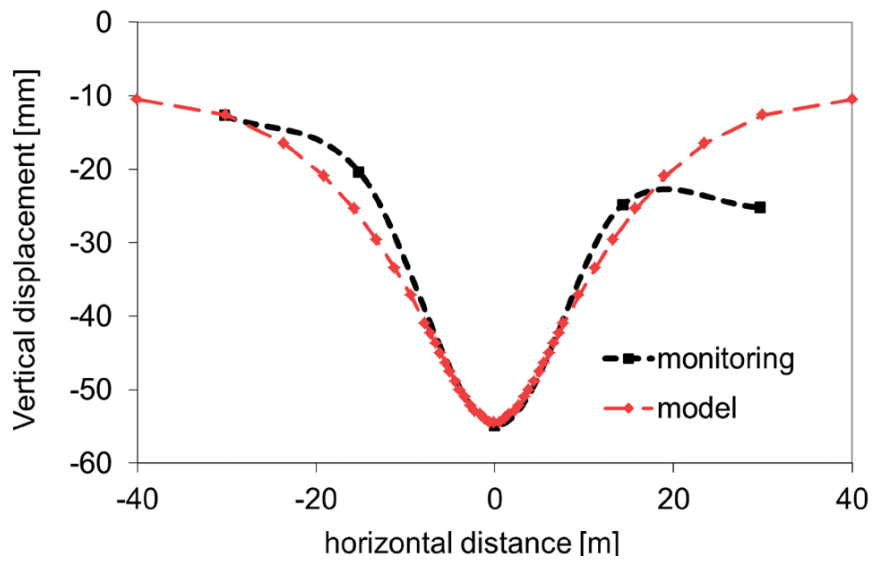


Figure 4. Distributions of vertical and horizontal displacements around the tunnel as predicted by the geotechnical model.

a)



b)

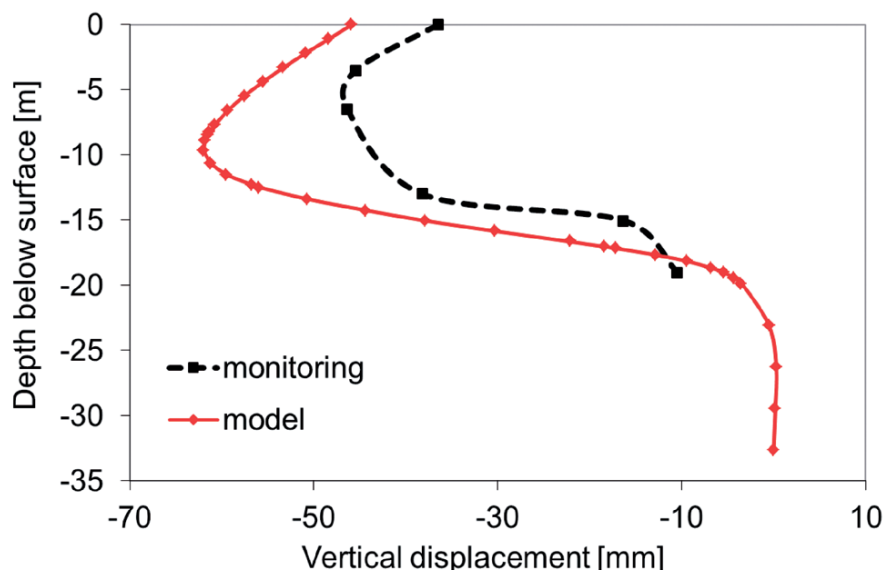


Figure 5. Comparison of results of a geotechnical model with monitoring data – (a) vertical surface displacement, (b) distribution of vertical displacement with depth in a vicinity of the tunnel.

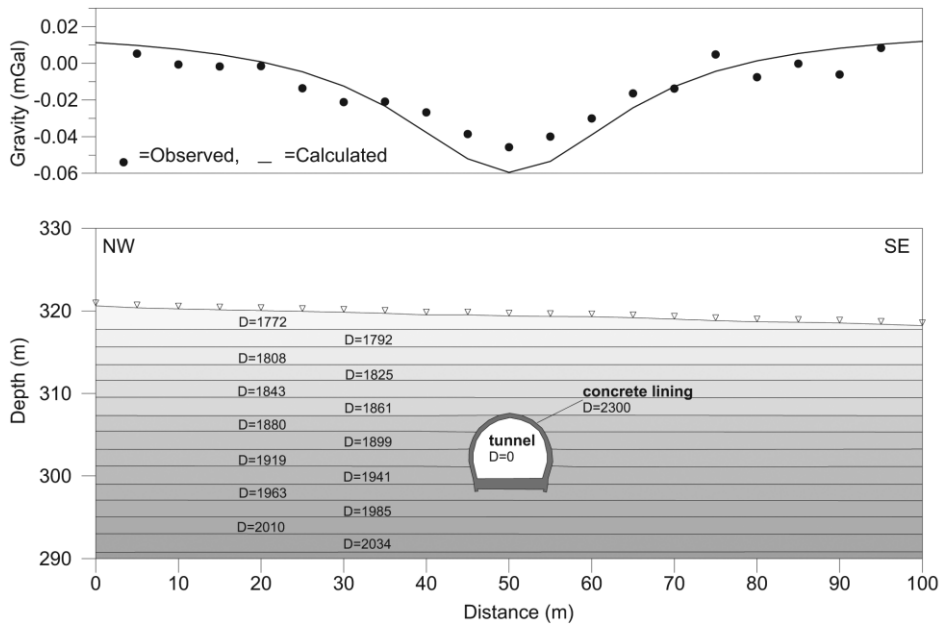


Figure 6. Model 1. Densities D [kg/m^3] are derived from measurements of borehole samples in soil mechanics laboratory (Fig. 3b). Amplitude of observed anomaly is -0.046 mGal, amplitude of calculated anomaly is -0.060 mGal, error of modelling is 0.009 mGal.

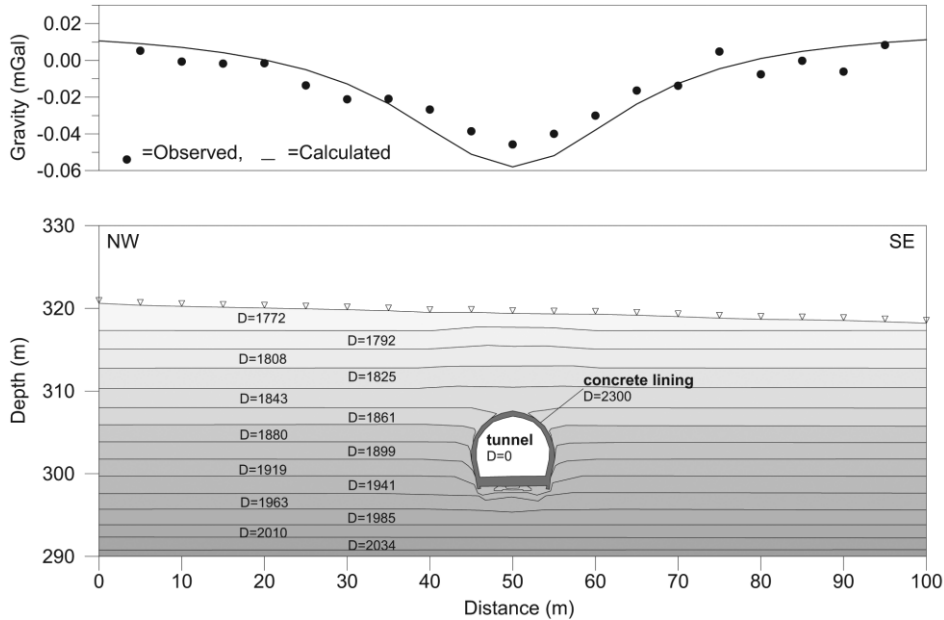


Figure 7. Model 2. Densities D [kg/m^3] are derived from measurements of borehole samples in soil mechanics laboratory (Fig 3b). Deformation zone around the tunnel is modeled according to the results of geotechnical modelling. Amplitude of observed anomaly is -0.046 mGal, amplitude of calculated anomaly is -0.059 mGal, error of modelling is 0.008 mGal.

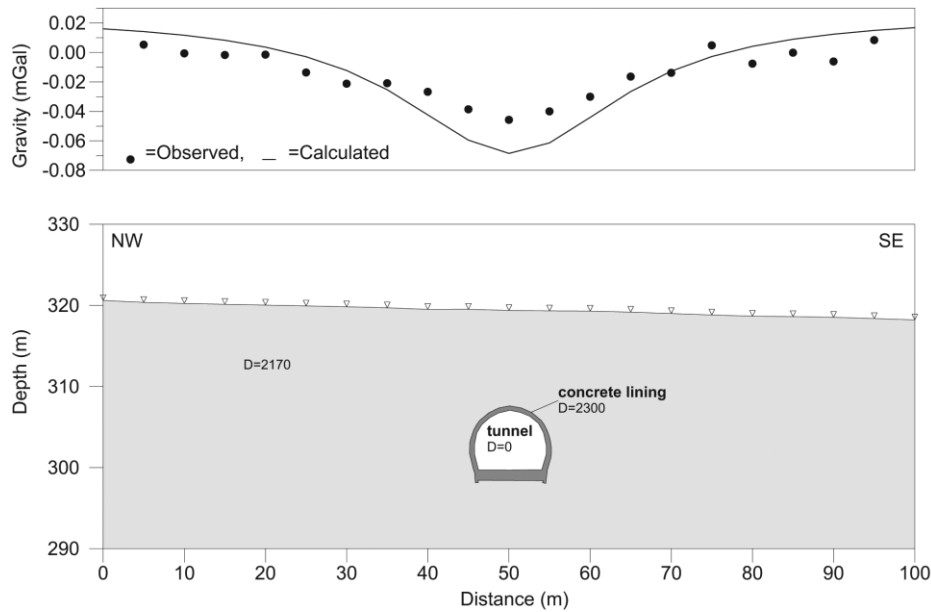


Figure 8. Model 3. Constant density of clays D [kg/m^3] is derived from measurements of borehole samples in rock density laboratory by “triple weighing” method (Fig. 3a). Amplitude of observed anomaly is -0.046 mGal, amplitude of calculated anomaly is -0.068 mGal, error of modelling is 0.013 mGal.

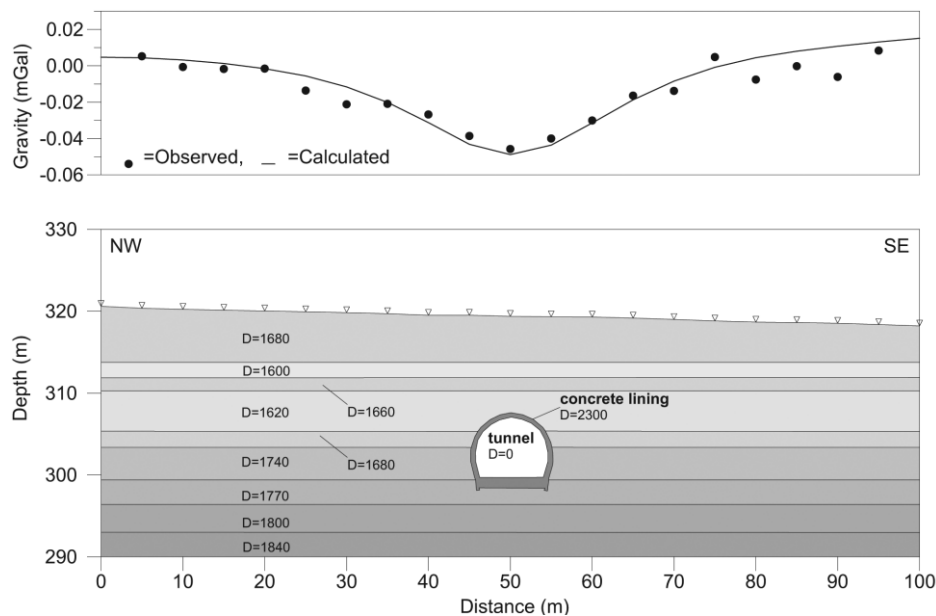


Figure 9. Model 4. Densities D [kg/m^3] are derived from gamma-gamma well log (Fig. 3c). Amplitude of observed anomaly is -0.046 mGal, amplitude of calculated anomaly is -0.049 mGal, error of modelling is 0.006 mGal.

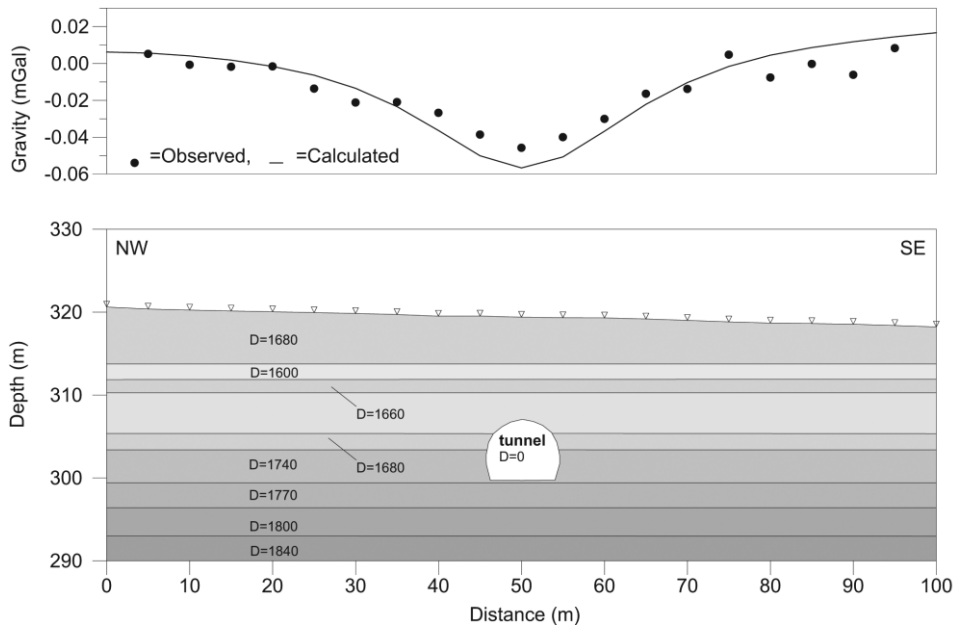


Figure 10. Model 5. The same as the model in Fig. 9, but the gravity effect of tunnel lining is omitted. Amplitude of observed anomaly is -0.046 mGal, amplitude of calculated anomaly is -0.057 mGal, error of modelling is 0.009 mGal.

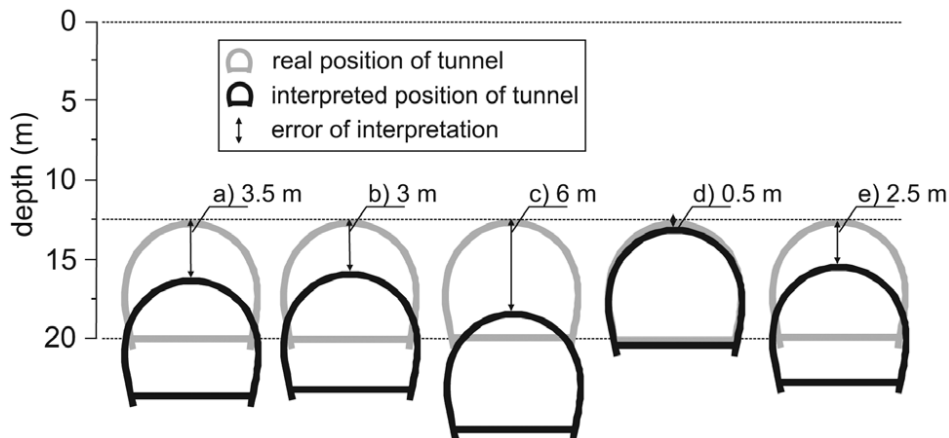


Figure 11. Errors of interpretation for different density models. Interpreted positions of the tunnel assuming the optimal fit between the observed and calculated data for the respective models. a) Model 1 – Fig. 6 (densities from soil mechanics laboratory), b) Model 2 – Fig. 7 (densities from soil mechanics laboratory and deformation zone), c) Model 3 – Fig. 8 (“triple weighing” laboratory method), d) Model 4 – Fig. 9 (densities from gamma-gamma well logging), e) Model 5 – Fig. 10 (densities from gamma-gamma well logging, tunnel lining omitted).

Tables

Table 1. Parameters of the hypoplastic model calibrated using the performed experimental data.

φ_c	λ^*	κ^*	N	r
18.0°	0.103	0.032	1.24	0.4

Table 2. Parameters of the very small strain extension of the hypoplastic model taken over from Svoboda *et al.* (2010).

m_R	m_T	R	β_r	χ
15	15	0.0001	0.2	0.8